THE JOURNAL OF PHYSICAL CHEMISTRY A

 VOLUME 108, NUMBER 29, JULY 22, 2004

LETTERS

Cascaded Energy Redistribution upon O−H Stretching Excitation in an Intramolecular Hydrogen Bond

Karsten Heyne,* Erik T. J. Nibbering, and Thomas Elsaesser

Max-Born-Institut für Nichtlineare Optik und Kurzzeitspektroskopie, Max-Born-Strasse 2A, D-12489 Berlin, Germany

Milena Petković and Oliver Kühn

Freie Universität Berlin, Institut für Chemie, Physikalische und Theoretische Chemie, Takustrasse 3, D-14195 Berlin, Germany

Received: March 26, 2004; In Final Form: May 25, 2004

Femtosecond two-color pump−probe experiments in the mid-infrared range demonstrate that excitation energy of the hydrogen-bonded O−H stretching oscillator of phthalic acid monomethyl ester is redistributed on a subpicosecond time scale along the O−H bending vibration. The O−H stretching and O−H bending lifetimes are 220 and 800 fs, respectively. Quantum dynamical model calculations of the energy flow induced by O−H stretching excitation reveal a relaxation mechanism involving cascaded energy redistribution along the O−H bending vibration and two O−H out-of-plane deformation modes at ∼700 and 800 cm^{-1}.

Vibrational excitation of a molecule in the condensed phase initiates relaxation processes by which the vibrational excess energy initially present in a particular mode is redistributed toward other modes (intramolecular vibrational redistribution, IVR) and/or dissipated to modes of the surrounding solvent (vibrational energy relaxation, VER).[1,2] For such processes, both intramolecular (e.g., anharmonic) couplings and interactions with the surrounding are relevant.[3−5] Understanding the pathways of IVR and VER is fundamentally important, because these have a key role in chemical reactions.

Hydrogen bonding is a local interaction present in many (bio)-molecular structures and in liquids. Vibrational relaxation of hydrogen-bonded systems has been studied to some extent without, however, reaching a consistent picture of relaxation pathways and time scales. Experimental studies of population relaxation of hydrogen-bonded O−H stretching vibrations (ν_{OH}) have shown time scales that are substantially shorter than those for other vibrations. The ν_{OH} lifetime in weak hydrogen bonds, such as water or alcohols, is ∼1 ps, whereas the lifetime decreases to several hundreds of femtoseconds for medium−strong hydrogen bonds. This lifetime shortening has been ascribed to efficient relaxation channels caused by (i) strong coupling due to Fermi resonances of the $\upsilon = 1$ state of the ν_{OH} oscillator with combination or overtone levels, in particular, the $\upsilon = 2$ level of the O−H bending mode (δ_{OH});[3,6,7] (ii) energy transfer into low-frequency hydrogen bond modes affecting the hydrogen bond length;[8] or (iii) cleavage of the hydrogen bond by excitation of the ν_{OH} vibration and subsequent reformation of the hydrogen bond on a longer time scale.[9,10] In most cases studied so far, a clear separation of such mechanisms and a quantitative analysis of their relative contributions to relaxation have not been possible.

In this paper, we present a study of O−H stretching relaxation in a medium−strong intramolecular hydrogen bond of well-defined geometry. Phthalic acid monomethyl ester (PMME-H,

* Author to whom correspondence should be addressed. Phone: +493063921410. Fax: +493063921429. E-mail address: heyne@mbi-berlin.de.

10.1021/jp048653f CCC: $27.50
Published on Web 06/30/2004

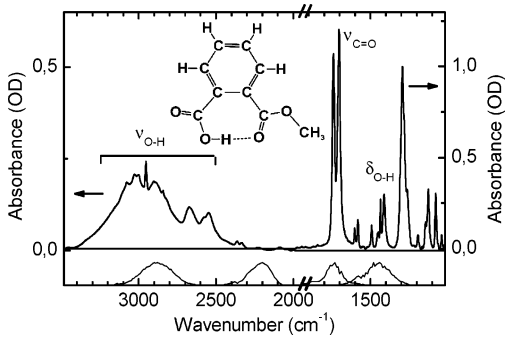

Figure 1. Infrared steady-state absorbance spectrum of phthalic acid monomethyl ester (PMME-H) dissolved in CCl_4 (solvent-subtracted spectrum). The O−H stretching vibration (ν_{OH}) absorbs at ∼3000 cm^{-1}, the C═O stretching (ν_{CO}) at 1740 cm^{-1}, and the O−H bending (δ_{OH}) at 1415 cm^{-1}. Spectra of pump and probe pulses are shown in the lower part, and the molecular structure of PMME-H is shown as an inset.

Figure 1) in nonpolar solution represents a model system for medium−strong hydrogen bonds[11−15] and is investigated in femtosecond two-color infrared pump−probe experiments concentrating on O−H stretching and O−H bending excitations. The vibrational lifetimes of the $v(\nu_{OH}) = 1$ and $v(\delta_{OH}) = 1$ states have values of 220 and 800 fs, respectively. We demonstrate that the intramolecular vibrational energy redistribution pathway from the ν_{OH} to the δ_{OH} oscillator is an efficient relaxation channel for this intramolecular hydrogen bond system. We perform quantum chemical and quantum dynamical calculations to analyze which modes of PMME-H couple most strongly to the ν_{OH} and δ_{OH} modes. A five-dimensional (5D) model comprising this subset of modes in PMME-H is used to calculate the cascaded vibrational energy flow that leads to fast relaxation of both the $v(\nu_{OH}) = 1$ and $v(\delta_{OH}) = 1$ states.

For our experiments, PMME-H was dissolved in CCl_4 with a concentration of 0.2 M (sample thickness of 0.01 cm, temperature of 293 K). Vibrational dynamics were studied in pump−probe experiments with independently tunable 100-fs pulses. Nonlinear vibrational absorption was monitored using different pump−probe schemes. After excitation of the O−H stretching (ν_{OH}), C═O stretching (ν_{CO}), or O−H bending (δ_{OH}) mode (see Figure 1), the δ_{OH} oscillator was probed. We estimate the ratio of excitation probability of ν_{OH} vs ν_{CH} (using the absorption cross sections and spectral bandwidth of the pump pulses) to be 100:7, in accordance with the magnitude of the induced transient absorbance changes observed at the spectrally separated δ_{OH} and δ_{CH} transitions. In addition, measurements with exciting and probing of ν_{OH} were performed. Pump and probe pulses were generated in two separate parametric sources with a repetition rate of 1 kHz. The pump pulse excites ∼2% of the molecules in the sample volume. After interaction with the sample, the weak probe pulses were spectrally dispersed and detected by a HgCdTe detector array (resolution of 5 cm^{-1}).

Results of measurements performed with ν_{OH} pumping and probing are presented in Figure 2a. The spectrally integrated change of absorbance is plotted as a function of the time delay between pump and probe pulses centered at 3000 and 2200 cm^{-1}, respectively. At this probe frequency, a contribution of the $v(\nu_{OH}) = 0 \rightarrow 1$ fundamental transition to the nonlinear absorption change is negligible. The increase of absorption is due to the $v(\nu_{OH}) = 1 \rightarrow 2$ transition with a very broad spectral envelope,[16,17] which displays an instantaneous rise and a fast decay superimposed by oscillatory signals. The data are well-reproduced by a kinetic model that consists of an instantaneous rise and an exponential decay with a time constant of 220 ± 80 fs, convoluted with the cross correlation of pump and probe

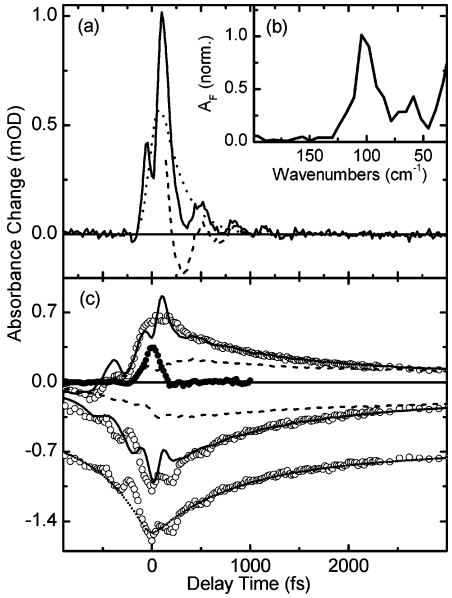

Figure 2. (a) Time-dependent change of the O−H stretch absorbance $\Delta A = -\log(I/I_0)$, as a function of the time delay between the pump at 3000 cm^{-1} and the probe pulse at 2200 cm^{-1} (solid line; I and I_0 represent the sample transmission with and without excitation, respectively) and the numerical fit of the data (dotted line). The oscillatory signal contribution (dashed line) was derived by subtracting the numerical fit from the measured ΔA value. (b) Normalized Fourier intensity of the oscillatory signal. (c) Transients of the O−H bending absorbance detected at 1390 cm^{-1} (positive signals) and 1415 cm^{-1} (negative signals) after exciting the O−H stretching (solid lines), the C═O stretching (dashed lines), and the O−H bending (circles) vibrations. Dotted line in panel c represents a simulation of bleaching by a kinetic model with a rise time of 550 fs and decay times of 0.8 and 7 ps, convoluted with the system response. Simulation and a replica of the transient measured at 1415 cm^{-1} are downshifted for separation. Solid circles in panel c represent a cross correlation of pump and probe pulses.

(see Figure 2a). It has been demonstrated by three pulse photon echo peak shift experiments that spectral diffusion within the O−H stretching band is negligible.[13] Thus, the observed kinetics mainly reflect the decay of the $v(\nu_{OH}) = 1$ state. On top of the incoherent dynamics, oscillatory signals with a frequency of 100 cm^{-1} (see Figure 2b) are detected, which indicate the coherent wave packet motion of the hydrogen bond out-of-plane low-frequency mode (γ_{HB}).[12]

In Figure 2c, we present transients measured in the spectral range of the O−H bending absorption upon exciting the $v(\nu_{OH}) = 0 \rightarrow 1$ transition at 2900 cm^{-1} (solid lines), $v(\nu_{CO}) = 0 \rightarrow 1$ transition at 1740 cm^{-1} (dashed lines) and $v(\delta_{OH}) = 0 \rightarrow 1$ transition at 1400 cm^{-1} (circles). The ordinate scale gives the absorbance change observed for δ_{OH} excitation (circles). The signal amplitudes measured with ν_{OH} and ν_{CO} excitation were divided by respective factors of 4.2 and 3.0, to match all amplitudes at a delay time of 3 ps. For a spectrally resolved detection of the probe, one finds transient bleaching signals of the steady-state (δ_{OH}) absorption at 1415 cm^{-1} (negative signals in Figure 2c). The slow rise of the bleaching signal at negative delay times is due to the perturbed free induction decay of the vibrational polarization, which is generated by the probe pulse and perturbed by the subsequent pump pulse.[18] This rise is well-reproduced by an exponential fit with a time constant of 550 fs (dotted line in Figure 2c, bottom), corresponding to the transverse homogeneous dephasing time (T_2) of the homogeneously broadened $v(\delta_{OH}) = 0 \rightarrow 1$ transition (width of ∼18 cm^{-1}). Enhanced absorption is observed at lower frequencies, with a maximum at 1390 cm^{-1} (positive signals in Figure 2c).

The decay of the absorbance changes extends up to positive delay times of 30 ps (not shown) and is well-reproduced by time constants of 800 ± 100 fs and 7 ± 1 ps. In contrast, only slow kinetics of the (δ_{OH}) absorption is found upon excitation of the C=O stretching mode.

Direct excitation of the $v(\delta_{OH}) = 0 \rightarrow 1$ transition shows a simultaneous rise of bleaching (1415 cm^{-1}) and enhanced absorption (1390 cm^{-1}) and a fast decay to 30% of its maximal amplitude, followed by a slow decay (circles in Figure 2c). We attribute the fast 800-fs component to the decay of the $v(\delta_{OH}) = 1$ state, giving rise to stimulated emission (at 1415 cm^{-1}) and red-shifted excited-state absorption (at 1390 cm^{-1}), where the red shift originates from the δ_{OH} anharmonicity. The subsequent slow decay on a time scale of several picoseconds is due to the O−H bending fundamental transition transiently red-shifted by anharmonic coupling to other modes, which are populated through O−H bending relaxation.[19]

Transients measured upon excitation of the $v(\nu_{CO}) = 0 \rightarrow 1$ transition exhibit only the slow δ_{OH} kinetics (dashed lines in Figure 2c), indicating a negligible population transfer from ν_{CO} to δ_{OH}. In contrast, excitation of the $v(\nu_{OH}) = 0 \rightarrow 1$ transition results in very similar transients at 1415 and 1390 cm^{-1} (solid lines in Figure 2c), as observed upon O−H bending excitation. In particular, the pump−probe signals display the 800-fs component, indicating that the $v(\delta_{OH}) = 1$ state is populated. From the signal amplitudes and the fraction of molecules excited, one can estimate that >30% of the O−H stretching excitation energy relaxes through the O−H bending mode.

We now discuss our quantum chemical and quantum dynamical modeling of the vibrational energy flow in PMME-H. VER in solution is modeled using the system−bath approach of condensed-phase quantum dynamics.[20] Following refs 14 and15, we describe the intramolecular vibrational dynamics in terms of normal mode coordinates, whereas the solvent is modeled as an effective harmonic oscillator bath. The intramolecular potential is calculated using the DFT/B3LYP (6-31+G(d,p)) method.[21] We combine single point energies on a grid and 4th-order anharmonic force field calculations[22] with a potential that includes up to four mode correlations. From the analysis of the 4th-order anharmonic force field, we identify a 5D model for vibrational energy flow in PMME-H that includes the ν_{OH} and the δ_{OH} mode, the low-frequency hydrogen bond out-of plane mode γ_{HB}, and two modes (γ_{OH1} and γ_{OH2}) which both showing substantial O−H out-of-plane deformation character (Figure 3a). In regard to energy, combination transitions of γ_{OH1} and γ_{OH2} are similar to the δ_{OH} fundamental transition, and combination levels of γ_{OH1} and γ_{OH2} with the δ_{OH} mode are almost resonant with the $v(\nu_{OH}) = 1$ state.

The time scale separation between the γ_{HB} mode and the other four modes allows for the introduction of a diabatic basis, which diagonalizes the rotation-free Hamiltonian at the equilibrium position of the γ_{HB}-mode coordinate. These diabatic states can be characterized in terms of the zero-order states of the noninteracting anharmonic modes, having the quantum numbers ($v(\nu_{OH})$, $v(\delta_{OH})$, $v(\gamma_{OH1})$, and $v(\gamma_{OH2})$). The diabatic level scheme is illustrated in Figure 3b and 3c.

This 5D system is coupled to an intramolecular system and a solvent bath.[14,15] Two relaxation mechanisms are included: (i) the relaxation of the low-frequency mode via one-quantum solvent mode transitions (the parameters are taken from ref 15, where the relaxation rate was determined to $(1.67)^{-1}$ ps for the lowest pair of γ_{HB} states), and (ii) for the relaxation of modes γ_{OH1} and γ_{OH2}, we assume a third-order mechanism to be effective (which involves energy release into one quantum of an intramolecular bath mode of comparable frequency plus one quantum of a solvent mode; the spectral density is taken to be the same as for mechanism (i)).[15] The system−bath coupling constants for γ_{OH1} and γ_{OH2} are assumed to be equal and are adjusted to give a $v(\nu_{OH}) = 1$ state lifetime of 200 fs. The population dynamics of this dissipative model is calculated using the Redfield equations in the Bloch limit.[14,20]

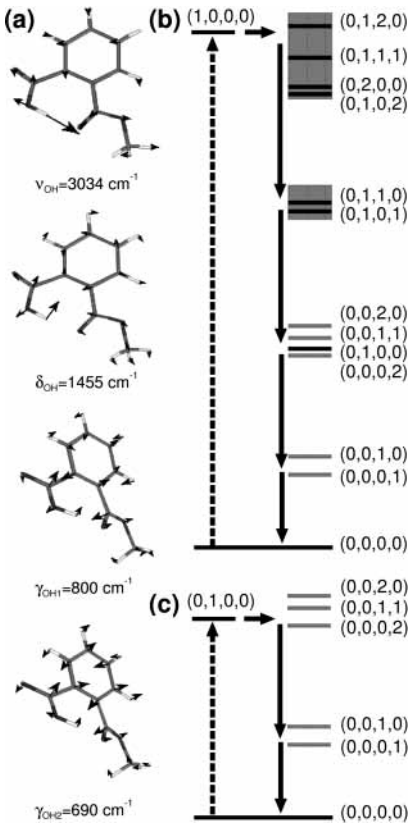

Figure 3. (a) Normal mode displacements and frequencies of the four modes comprising the diabatic basis. (b) Excitation of the OH-stretching fundamental transitions (dashed arrow) and relaxation pathway (solid arrow) within the diabatic level scheme. The higher overtone, as well as the combination transitions involving the modes ν_{OH1} and ν_{OH2}, are shown as gray rectangles. Panel c is the same as panel b, but for excitation of the OH-bending fundamental transition. Each level in panels b and c is dressed by coupled anharmonic potential curves of the low-frequency mode.

Calculated population dynamics after impulsive Franck−Condon-like excitation of the diabatic ground state wave packet into diabatic potentials of dominantly $v(\nu_{OH}) = 1$ and $v(\delta_{OH}) = 1$ character are presented in Figure 4a and 4b, respectively. Note that, for simplicity, we have neglected the diabatic state coupling for the excitation process. Figure 4a reveals that the dominant relaxation channel of the $v(\delta_{OH}) = 1$ state is not the $v(\delta_{OH}) = 2 \rightarrow 1$ transition, which is populated by, at most, 5% only during relaxation (not shown), but rather a pathway that involves the modes γ_{OH1} and γ_{OH2}. The energy relaxes from the O−H stretching excitation (1,0,0,0) directly into the almost-resonant combination states (0,1,1,1), (0,1,2,0), and (0,1,0,2) and then via the intermediate states (0,1,1,0) and (0,1,0,1) to the pure O−H bending mode (0,1,0,0) and eventually to the ground state (0,0,0,0). Relaxation of the O−H bending mode involves overtone and combination-tone states of the γ_{OH1} and γ_{OH2} modes (see Figure 4b). It is important to note that this cascaded model well-reproduces (i) the ratio of the $v(\nu_{OH}) = 1$ and $v(\delta_{OH}) = 1$ lifetimes and (ii) the measured decay of $v(\delta_{OH}) = 1$, both upon ν_{OH} excitation as well as upon δ_{OH} excitation, using the same set of parameters.

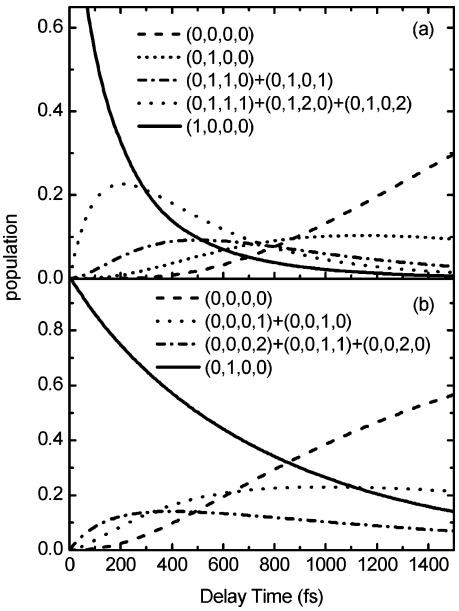

Figure 4. Diabatic state population dynamics after impulsive Franck−Condon-like excitation of the state dominated by the (a) OH-stretching and (b) OH-bending fundamental transitions.

We infer from our combined experimental and theoretical study that the strong Fermi resonance coupling of the O−H stretching vibration to combination and overtone levels is the dominant mechanism for efficient $v(\nu_{OH}) = 1$ relaxation in PMME-H. We can exclude the alternative relaxation mechanisms. Breaking of the hydrogen bonds upon ν_{OH} excitation would result in a significant red shift of the $v(\delta'_{OH}) = 0 \rightarrow 1$ and the $v(\delta'_{OH}) = 1 \rightarrow 2$ transition of the free O−H bending vibration. In contrast, the measured absorbance difference spectra and dynamics of the O−H bending vibration exhibit the same spectral features and lifetimes upon ν_{OH} and δ_{OH} excitation. Thus, we conclude that hydrogen bond breaking does not occur upon O−H stretching excitation. Anharmonic coupling to low-frequency hydrogen bond modes that modulate strongly the hydrogen bond distance is observed by the wave packet motion in the $v(\nu_{OH}) = 1$ state. We can exclude, however, an efficient relaxation mechanism from $v(\nu_{OH}) = 1$ state directly to the low-frequency modes, because of the poor ("Franck−Condon") overlap of the wave functions.

In summary, we have demonstrated that the fast energy relaxation of the O−H stretching vibration (ν_{OH}) in a medium−strong intramolecular hydrogen bond originates from a cascaded energy redistribution over the O−H bending mode (δ_{OH}) and other accepting modes at ∼700 and 800 cm^{-1}. This conclusion is drawn from a two-color pump−probe study of nonlinear vibrational absorption in the range of the ν_{OH} and δ_{OH} modes and calculations using a relaxation mechanism that involves simultaneous energy release into intramolecular and solvent modes.

Acknowledgment. We thank the DFG (Sfb 450) and the Fonds der Chemischen Industrie (O.K.) for financial support.

References and Notes

(1) Elsaesser, T.; Kaiser, W. *Annu. Rev. Phys. Chem.* **1991**, *42*, 83.
(2) Owrutsky, J. C.; Raftery, D.; Hochstrasser, R. M. *Annu. Rev. Phys. Chem.* **1994**, *45*, 519.
(3) Rey, R.; Møller, K. B.; Hynes, J. T. *Chem. Rev.* **2004**, *104* (4), 1915−1928.
(4) Lawrence, C. P.; Skinner, J. L. *J. Chem. Phys.* **2003**, *119*, 1623.
(5) Fayer, M. D. *Ultrafast Infrared and Raman Spectroscopy*; Marcel Dekker: New York, 2001.
(6) Deàk, J. C.; Rhea, S. T.; Iwaki, L. K.; Dlott, D. D. *J. Phys. Chem. A* **2000**, *104*, 4866.
(7) Petković, M.; Kühn, O. *J. Phys. Chem. A* **2003**, *107*, 8458.
(8) Nienhuys, H.-K.; Woutersen, S.; van Santen, R. A.; Bakker, H. J. *J. Chem. Phys.* **1999**, *111*, 1494.
(9) Graener, H.; Ye, T. Q.; Lauberau, A. *J. Chem. Phys.* **1989**, *90*, 3413.
(10) Asbury, J. B.; Steinel, T.; Stromberg, C.; Gaffney, K. J.; Piletic, I. R.; Goun, A.; Fayer, M. D. *Chem. Phys. Lett.* **2003**, *374*, 362.
(11) Madsen, D.; Stenger, J.; Dreyer, J.; Hamm, P.; Nibbering, E. T. J.; Elsaesser, T. *Bull. Chem. Soc. Jpn.* **2002**, *75*, 909.
(12) Stenger, J.; Madsen, D.; Dreyer, J.; Nibbering, E. T. J.; Hamm, P.; Elsaesser, T. *J. Phys. Chem. A* **2001**, *105*, 2929.
(13) Stenger, J.; Madsen, D.; Dreyer, J.; Hamm, P.; Nibbering, E. T. J.; Elsaesser, T. *Chem. Phys. Lett.* **2002**, *354*, 256.
(14) Kühn, O. *J. Phys. Chem. A* **2002**, *106*, 7671.
(15) Kühn, O.; Naundorf, H. *Phys. Chem. Chem. Phys.* **2003**, *5*, 79.
(16) Bakker, H. J.; Nienhuys, H. K.; Gallot, G.; Lascoux, N.; Gale, G. M.; Leicknam, J.-C.; Bratos, S. *J. Chem. Phys.* **2002**, *116*, 2592.
(17) Heyne, K.; Huse, N.; Dreyer, J.; Nibbering, E. T. J.; Elsaesser, T.; Mukamel, S. *J. Chem. Phys.* **2004**, in press.
(18) Wynne, K.; Hochstrasser, R. M. *Chem. Phys.* **1995**, *193*, 211.
(19) Heyne, K.; Huse, N.; Nibbering, E. T. J.; Elsaesser, T. *Chem. Phys. Lett.* **2003**, *382*, 19.
(20) May V.; Kühn, O. *Charge and Energy Transfer Dynamics in Molecular Systems*, 2nd Revised and Enlarged Edition; Wiley−VCH: Weinheim, Germany, 2004.
(21) Frisch, M. J.; Trucks, G. W.; Schlegel, H. B.; Scuseria, G. E.; Robb, M. A.; Cheeseman, J. R.; Zakrzewski, V. G.; Montgomery, J. A., Jr.; Stratmann, R. E.; Burant, J. C.; Dapprich, S.; Millam, J. M.; Daniels, A. D.; Kudin, K. N.; Strain, M. C.; Farkas, O.; Tomasi, J.; Barone, V.; Cossi, M.; Cammi, R.; Mennucci, B.; Pomelli, C.; Adamo, C.; Clifford, S.; Ochterski, J.; Petersson, G. A.; Ayala, P. Y.; Cui, Q.; Morokuma, K.; Malick, D. K.; Rabuck, A. D.; Raghavachari, K.; Foresman, J. B.; Cioslowski, J.; Ortiz, J. V.; Stefanov, B. B.; Liu, G.; Liashenko, A.; Piskorz, P.; Komaromi, I.; Gomperts, R.; Martin, R. L.; Fox, D. J.; Keith, T.; Al-Laham, M. A.; Peng, C. Y.; Nanayakkara, A.; Gonzalez, C.; Challacombe, M.; Gill, P. M. W.; Johnson, B. G.; Chen, W.; Wong, M. W.; Andres, J. L.; Head-Gordon, M.; Replogle, E. S.; Pople, J. A. *Gaussian 98*, revision A.11; Gaussian, Inc.: Pittsburgh, PA, 1998.
(22) Császár, A. G. In *Encyclopedia of Computational Chemistry*; Schleyer, P. v. R., ed.; Wiley: Chichester, U.K., 1998; p 13.